Determination of Solvation Layer Thickness by a Magnetophotonic Approach

Le He, Yongxing Hu, Mingsheng Wang, and Yadong Yin*

Department of Chemistry, University of California, Riverside, California 92521, United States

ABSTRACT

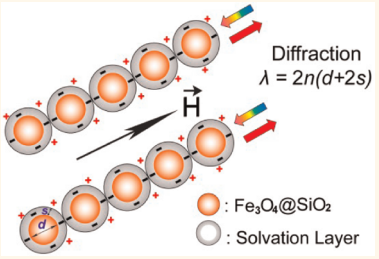

Derjaguin—Landau—Verwey—Overbeek (DLVO) theory fails in explaining the superior stability of colloid particles in aqueous suspensions under conditions of high ionic strengths where electrostatic forces are effectively screened. Accumulating evidence shows that the formation of a thin rigid layer of solvent molecules in the vicinity of a colloidal particle surface provides an additional repulsive interaction when the interparticle distance is reduced to several nanometers. The effective determination of the thickness of the solvation layer however remains a challenge. Here, we demonstrate a simple yet powerful magnetophotonic technique that can be used to study the thickness of the solvation layers formed on the colloidal silica surface in various polar solvents. A relationship between the hydrogen-bonding ability of the solvents and the thickness of solvation layer on colloidal silica surfaces has been identified; this observation is found to be consistent with the previously proposed hydrogen-bonding origin of the solvation force.

KEYWORDS: solvation layer · repulsion · electrostatic interaction · magnetic nanoparticles · silica · colloids · diffraction

The forces between colloidal particles play important roles in determining the stability of colloidal suspensions. Derjaguin—Landau—Verwey—Overbeek (DLVO) theory, which considers the sum of the London—van der Waals attraction and the electrostatic repulsion between two particles, has been widely used to explain and predict the stability of colloids in liquid medium.[1−3] The electrostatic repulsive interaction between colloids is believed to provide an energy barrier against particle aggregation. However, DLVO theory fails in explaining the superior stability of silica colloids in aqueous suspensions under conditions of high ionic strength where the electrostatic forces are effectively screened.[4,5] Recent studies have shown that another repulsive force, the solvation force, may become dominant when the distance between silica surfaces drops in the range of several nanometers.[6−13] While the physical origin of this strong short-range force is still under debate,[10,14,15] it has been mostly attributed to the formation of a thin rigid layer of solvent molecules in the vicinity of silica surfaces through hydrogen bonding.[9,13,16,17] According to this theory, a thicker solvation layer and stronger interparticle solvation force should develop for silica colloids in solvents with stronger hydrogen-bonding abilities. Yoon and Vivek studied the effects of adding short-chain alcohols into aqueous silica suspensions on the solvation force between silica surfaces.[18] They attributed the decrease in solvation force to the dehydration of the silica surface with the addition of short-chain alcohols and claimed that the solvation force may even disappear in a 15% methanol aqueous solution. However, the argument that the replacement of water with methanol results in the complete disappearance of a solvation force contradicts the hydrogen-bonding theory as methanol may also participate in the hydrogen bonding network and contribute to the solvation repulsions. Indeed, the solvation force between silica surfaces was found to exist in many nonaqueous solvents with strong hydrogen-bonding ability.[19] Further systematic studies are apparently needed to clarify the apparent contradictions existing in literature.

While the fundamental understanding of the colloidal interactions has been advanced with the realization of many force measurement tools, most experiments were carried out using involved techniques and instrumentation, such as atomic force microscopy (AFM) or a surface force apparatus (SFA).[9,20] It would be a great advantage to study the solvation force between colloidal particles using simple techniques with easily accessible setups. Bibette *et al*. developed a

* Address correspondence to yadongy@ucr.edu.

Received for review February 19, 2012 and accepted April 20, 2012.

Published online April 20, 2012
10.1021/nn3007288

magnetic chaining technique to directly probe repulsive forces between colloidal particles in aqueous suspensions.[21−24] Upon the application of an external magnetic field, monodispersed emulsion droplets containing superparamagnetic iron oxide nanocrystals self-assemble into chain structures with a periodic arrangement as driven by the force balance between magnetic dipole−dipole attraction and different interparticle repulsions. As the distance between neighboring particles can be derived from the wavelength of the optical diffraction of the periodic assemblies through Braggs' law, different long-range and short-range repulsive forces have been studied.[22,23,25] Compared to conventional techniques, this method allows simple control over the interparticle distance, and thus the force−distance law can be conveniently derived. However, the apparent drawbacks of the approach include the lack of long-term stability of the structures from emulsion droplets, and the complicated and time-consuming steps needed for the fabrication of uniform emulsion droplets due to the involvement of multiple size-selection processes. More importantly, the surface property of the droplet is determined by the surfactants used, which complicates the application of the technique for the study of many other short-range interactions such as the solvation force.

Recently, we have extended this magneto-photonic effect to the development of responsive photonic structures with widely, rapidly and reversibly magnetically tunable structural colors in the visible and near-infrared spectrum by using nanostructured superparamagnetic magnetite (Fe_3O_4) colloidal nanocrystal clusters.[26] Engineering the surface of the magnetic colloids with a layer of silica (Fe_3O_4@SiO_2) through a simple sol−gel process improves their compatibility with many other nonaqueous solvents such as alkanol solutions[27] and UV curable resins.[28−30] In this work, we take advantage of the optical response of the core−shell magnetic colloids under magnetic fields to study the thickness of solvation layers formed when the colloidal silica surface is covered by different solvents. The key to the successful measurement of the thickness of the solvation layer is the effective screening of the electrostatic force so that the neighboring particles interact with each other through the repulsion resulting from the overlap of solvation layers, which balances the magnetically induced attraction and forms ordered assemblies. The thickness of solvation layer can be then estimated by using Bragg's law. A relationship between the hydrogen-bonding ability of the solvents and the thickness of solvation layer on Fe_3O_4@SiO_2 colloidal surface has been identified, which is consistent with the prior understanding of a hydrogen-bonding origin of the solvation force. Compared to conventional complex techniques, our magneto-photonic strategy represents an easily accessible method with a simple and inexpensive setup that produces consistent results.

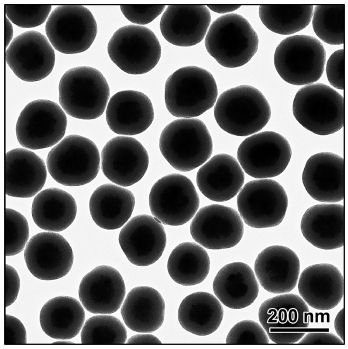

Figure 1. Typical TEM image of a Fe_3O_4@SiO_2 sample with an average diameter of 175 nm (115 nm core diameter/ 30 nm shell thickness).

RESULTS AND DISCUSSION

Monodisperse polyelectrolyte-capped superparamagnetic Fe_3O_4 colloidal nanocrystal clusters (CNCs) were prepared through a one-pot high-temperature precipitation reaction,[31] then coated with a layer of silica with controlled thickness through a sol−gel process.[27] After silica coating, the Fe_3O_4@SiO_2 core−shell particles can be dispersed in water and many nonaqueous polar solvents such as alcohols. As shown in the transmission electron microscopy image in Figure 1, the silica coating process improves the monodispersity of the particles and yields more spherical particles, facilitating more accurate measurements. Figure 2 illustrates the basic principle in determining the thickness of the solvation layer on the surface of colloidal Fe_3O_4@SiO_2 particles. The Fe_3O_4@SiO_2 particles self-assemble into dynamic photonic chains in the external magnetic field when the magnetically induced dipole−dipole attraction is balanced with interparticle repulsions. When the electrostatic force is effectively screened, the solvation force between the Fe_3O_4@SiO_2 surfaces dominates at the separation of a few nanometers, where the thin rigid solvation layer contacts, to balance the magnetically induced interparticle attraction. The diffraction of the photonic chains follows the Bragg's Law $\lambda = 2n(d + 2s) \sin \theta$, where λ is the diffraction wavelength, n the refractive index of the suspension, d the overall diameter of Fe_3O_4@SiO_2 particles, s the thickness of solvation layer, and the Bragg angle, $\theta = 90°$.[32,33] The diffraction wavelength (λ) can be measured using a spectrometer operated in reflectance mode, and the diameter of Fe_3O_4@SiO_2 particles can be identified by TEM while the refractive index of the suspensions can be measured. Finally, the thickness of the solvation layer (s) can be calculated using Bragg's law.

In our earlier efforts to estimate solvation layer thickness,[27] we were not able to completely eliminate the electrostatic repulsion and our values were not consistent with those obtained using force measurement techniques, although they seem to fit estimations based on rheological arguments.[34,35] It is well-known

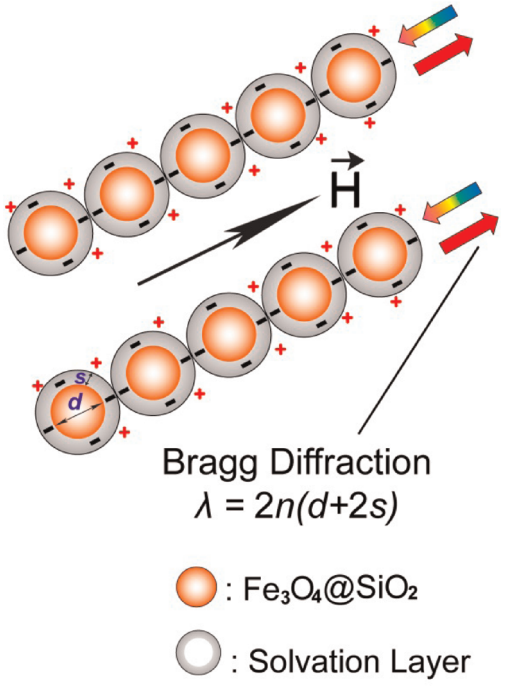

Figure 2. Schematic illustration of the magnetic assembly strategy to determine the thickness of the solvation layer (*s*) on the surface of Fe_3O_4@SiO_2 colloidal particles. In an external magnetic field, the Fe_3O_4@SiO_2 particles self-assemble into photonic chains along the magnetic field and Bragg-diffracted visible light. When the electrostatic force is effectively screened, the solvation layers contact and produce a repulsive force to balance the magnetic attraction between the colloids. The thickness of solvation layer (*s*) can be calculated using the Bragg equation with the effective refractive index (*n*), the diameter of colloids (*d*), and the measured wavelength (λ) of diffraction of the chains.

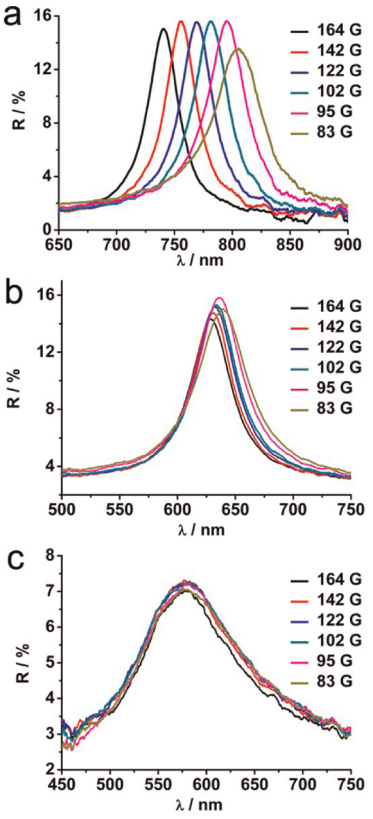

Figure 3. Reflection spectra from a 50% water–ethanol suspension of 208 nm (142 nm core diameter/33 nm shell thickness) Fe_3O_4@SiO_2 particles with the NaCl concentration of (a) 10^{-5} mol/L, (b) 0.01 mol/L, and (c) 0.025 mol/L in response to an external magnetic field with varying strengths.

that the interaction range of electrostatic forces can be characterized by the Debye length $\kappa^{-1} = (\epsilon k_B T/2000 N_A e^2 I)^{1/2}$, where ϵ is the dielectric constant, K_B is Boltzmann's constant, T is the absolute temperature, N_A is Avogadro's number, e is the elementary charge, and I is the ionic strength.[36] When the ionic strength of the water solution reaches 0.05 M, the electrostatic force between silica surfaces could be effectively screened and the solvation force starts to dominate the interparticle repulsion.[5] On the other hand, as reported by Grabbe and Horn, a repulsive force, dominant at short ranges between silica surfaces in aqueous solutions, is independent of NaCl concentrations up to 0.1 M.[9] Utilizing the difference in sensitivity to ionic strength of the solution between the electrostatic force and the solvation force, it is possible to selectively screen the electrostatic force between silica surfaces while keeping the solvation force unaffected.

The Fe_3O_4@SiO_2 particle dispersion in a 50% water–ethanol (volume fraction) solution was chosen as a model system to test the effect of electrolyte concentration on the interparticle repulsive forces. Figure 3 shows the reflectance spectra of a sample with a diameter of 208 nm (142 nm core diameter/33 nm shell thickness) in response to different external magnetic fields. When the ionic strength is low, the long-range electrostatic force dominates the repulsion between Fe_3O_4@SiO_2 particles so that the diffraction peak can be widely tuned by enhancing the strength of the magnetic field from 83 G to 164 G while the interparticle spacing decreases from ~90 to ~60 nm (Figure 3a). When the concentration of NaCl increases to 0.01 M in a 50% water–ethanol mixture, the diffraction blue-shifts relative to the above case in the same magnetic fields. The interparticle spacing only changed slightly from ~28 to ~24 nm (Figure 3b), indicating that the electrostatic force becomes much weaker but still dominates the interparticle repulsion as evidenced by the relatively large interparticle spacing in comparison to the typical thickness of solvation layers (several nanometers). The decrease of the long-range repulsion due to higher electrolyte concentration can be accounted for by the classical DLVO theory as the electrical double layers were compressed by the absorbed counterions. By further increasing the concentration of NaCl to 0.025 M, the diffraction peak moved to even shorter wavelengths (Figure 3c). Meanwhile, both the diffraction peak position and the interparticle

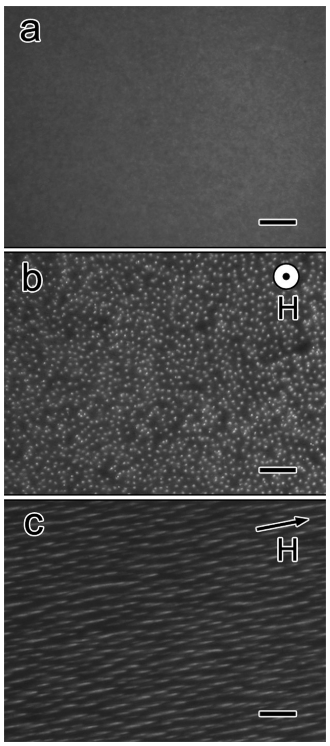

Figure 4. Optical microscope images showing the assembly of 208 nm (142 nm core diameter/33 nm shell thickness) Fe_3O_4@SiO_2 particles dispersed in a 50% water−ethanol suspension with NaCl concentration of 0.025 mol/L in a liquid film sandwiched between two glass slides under (a) no magnetic field, (b) magnetic field ~100 G parallel to the viewing angle, and (c) magnetic field ~100 G perpendicular to the viewing angle.

separation remained constant even as the magnetic field changed from 83 to 164 G. The interparticle spacing estimated using Bragg's equation was 6.6 nm, close to the range in which the solvation force became effective. The loss of tunability in diffraction wavelength also indicates the dominant repulsion came from the hard contact of the rigid solvation layer while the effectively screened double-layer repulsion became negligible. The diffraction peak finally disappeared due to the aggregation of chains when the magnetic field was further enhanced and the magnetic packing force became effective.

To confirm the formation of chainlike structures from Fe_3O_4@SiO_2 particles under the condition of screened electrostatic forces, their assembly behavior in response to the magnetic field was studied using an optical microscope operated in dark-field mode. Fe_3O_4@SiO_2 particles were well-dispersed in the 50% water−ethanol mixture with 0.025 M NaCl and cannot be clearly imaged due to the Brownian motion (Figure 4a). When a magnetic field of *ca.* 100 G was applied, Fe_3O_4@SiO_2 particles self-assembled into chains along the magnetic field (Figure 4b,c). The dynamic chains disappeared upon removal of the magnetic field with no obvious aggregation observed. When the field strength was increased to over 150 G, the chains

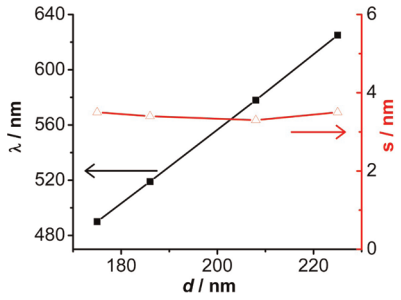

Figure 5. The diffraction wavelengths and the corresponding solvation layer thicknesses measured for different-sized Fe_3O_4@SiO_2 particles magnetically assembled in 50% water−ethanol mixtures containing 0.025 mol/L NaCl.

started to aggregate, consistent with the results from reflectance measurements. We also measured the solvation layer thickness on other Fe_3O_4@SiO_2 samples with diameters of 175 nm (115 nm core diameter/30 nm shell thickness), 186 nm (124 nm core diameter/32 nm shell thickness), and 225 nm (149 nm core diameter/38 nm shell thickness) in 50% water−ethanol mixtures with 0.025 M NaCl. The reflectance spectra of all samples showed a similar profile with no change of diffraction wavelength in response to the variation of magnetic fields within a certain strength range. More importantly, the estimated thicknesses of the solvation layers were found to be essentially the same for all of the samples (Figure 5), which confirms the reliability of our method, because according to the theory of hydrogen-bonding on the origin of solvation layers, the thickness of a solvation layer should be insensitive to the size of particles.

The above results demonstrate that our strategy of selectively screening the electrostatic force allows the estimation of solvation layer thickness on the surface of Fe_3O_4@SiO_2 particles through their magneto-photonic effect. Since the screening of the electrostatic force in aqueous solutions has been previously studied, here we demonstrate the application of the magneto-photonic method for the purpose of studying the effects of adding nonaqueous solvents on the thickness of the solvation layer on the silica surface. First, we studied how the solvation layer thickness changes upon the addition of ethanol. As shown in Figure 6a, the solvation layer on the surface of Fe_3O_4@SiO_2 particles was found to be thickest in pure water (~ 4.4 nm), and the addition of ethanol gradually contracted the solvation layer to a minimum of ~2 nm. Yoon and Vivek attributed the decrease in solvation layer to the dehydration of the silica surface with the addition of short-chain alcohols.[18] However, we believe the replacement of water with ethanol, which has relatively weaker hydrogen-bonding ability, might interfere with the hydrogen-bonding network so the overall rigid solvation layer would become thinner. Accordingly, increased replacement happens as the volume fraction of ethanol increases, further decreasing the solvation layer. Another phenomenon

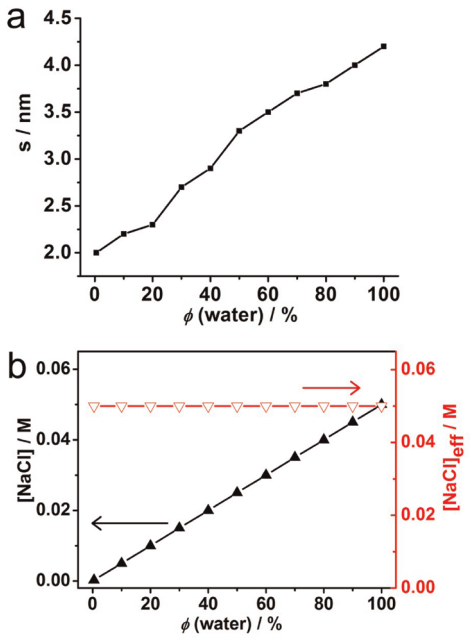

Figure 6. (a) The dependence of the solvation layer thickness (*s*) on the volume fraction of water, determined by the magneto-photonic method using Fe_3O_4@SiO_2 particles. (b) The dependence on concentration of NaCl required to effectively screen the interparticle electrostatic force on the volume fraction of water in water–ethanol mixtures. The concentration of NaCl on the left side is defined as moles of NaCl per volume of water–ethanol mixture while the value on the right side is defined as moles of NaCl per volume of water.

observed showed that the lowest concentration of NaCl required to effectively screen the electrostatic force follows a linear relationship with the volume fraction of water, but interestingly the effective concentration of NaCl in water was found to be constant (Figure 6b). The lowest concentration of NaCl for each solvent mixture is obtained through repetitive measurements of the same Fe_3O_4@SiO_2 solution but with increasing salt concentration until no change in diffraction spectra under variable magnetic fields. To estimate the solvation layer thickness in pure ethanol, in which salts tend to exhibit poor solubility, we simply added 2 μL of a 0.05 M NaCl aqueous solution into 1 mL of a CNC ethanol solution and found the electrostatic force can be readily screened.

Consistent with the theory that the solvation force results from the formation of a thin layer of solvent through hydrogen-bonding interactions, the addition of ethanol to Fe_3O_4@SiO_2 aqueous suspensions reduces the thickness of the solvation layer by replacing the water and interfering with the hydrogen-bonding network. With the expectation that the variation in hydrogen bonding abilities should result in changes in thickness of the solvation layer, we also studied the thickness change in different aqueous ethylene glycol (EG) solutions and found, interestingly, that they exhibit a different profile from the case of ethanol/water mixtures, first shrinking and then expanding

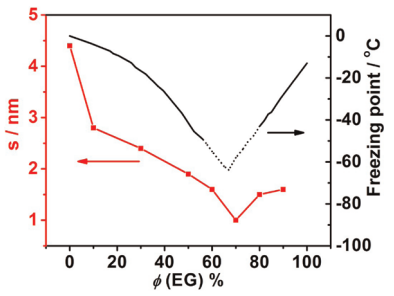

Figure 7. (Red) Plots of solvation layer thickness of Fe_3O_4@SiO_2 particles in water/EG mixtures. (Black) The dependence of the freezing point of water/EG mixtures on the volume fraction EG, plotted using literature data. The dotted curve represents the metastable freezing temperatures.

TABLE 1. Summary of Solvation Layer Thickness in Water and Various Aqueous Mixtures

solvent	molecular structure	refractive index	S (nm)
pure water	H_2O	1.3333	4.4
50% methanol	CH_3OH	1.3425	4.1
50% ethanol	C_2H_5OH	1.3578	3.5
50% 2-propanol	$(CH_3)_2CH-OH$	1.3658	2.6
50% EG	$HO-CH_2CH_2-OH$	1.3858	1.9
50% DEG	$(HO-CH_2CH_2)_2O$	1.3937	1.8
50% glycerol	$(HO-CH_2)_2CH-OH$	1.4084	1.8

with increasing EG concentration (Figure 7). The initial drop below the 70% volume fraction can be explained by the disruption of the solvation layer by replacing water with EG, which has much weaker hydrogen-bonding ability similar to the case of ethanol. However, unlike the case of ethanol/water mixture, the thickness of solvation layer increases when the EG concentration increases to above 70%. This concentration dependence is in fact consistent with the solid–liquid phase equilibrium of the EG/water mixture which has been plotted in the same graph by using data from literature.[37–39] A minimum freezing point at ~70% EG concentration indicates the most severe disruption of the hydrogen-bonding network, which now also leads to the thinnest solvation layer in the same volume fraction. When the volume fraction of EG is beyond 70%, the formation of the solvation layer might be progressively dominated by increased hydrogen bonding between EG molecules resulting in a slight increase of the solvation layer thickness.

Finally, we compared the dispersions of Fe_3O_4@SiO_2 particles in aqueous solutions of other nonaqueous solvents by keeping the volume fractions constant at 50%. Table 1 summarizes the results from different mixtures. For simple alcohols with only one hydroxyl group (R–OH), the thickness of solvation layer decreases with the increase of the chain length of the R group. The thickness in a methanol–water mixture is ~4.1 nm, which is close to the value in pure water (~4.4 nm). When the methyl group (CH_3–) is replaced

by an ethyl group (C_2H_5—) or isopropyl group ($(CH_3)_2CH$—), the solvation layer shrinks to 3.5 and 2.6 nm, respectively. Apparently, this trend is consistent with the decrease of the hydrogen-bonding ability of alcohols as their carbon chain lengths increase.[19] Compared to simple alcohols with relatively strong hydrogen bonding abilities, the decrease in the thickness of solvation layer is more obvious when using weak hydrogen bonding solvents such as EG, diethylene glycol (DEG), or glycerol. As a matter of fact, these solvent mixtures have been widely used as antifreezing agents since the mixture can severely disrupt hydrogen bonding and thus greatly depress the freezing point of the system. For example, the freezing point of 50% EG—water mixture is −39 °C, which is lower than that of pure water (0 °C) and pure EG (−13 °C). As expected, a more severe disruption to the hydrogen bonding network by the addition of EG to the solution to reach a 70% volume fraction further reduces the freezing point to below −51 °C, which is consistent with the observation of the thinnest solvation layer at the same volume fraction.

CONCLUSION

We report here a simple and easily accessible magneto-photonic method to study the thickness of solvation layer on colloidal silica surfaces in different polar solvents. By exposing uniform Fe_3O_4@SiO_2 colloidal particles dispersed in various solvents to a magnetic field, they are attracted to close contact with one another and self-align into 1D periodically arranged photonic chains that diffract visible light consistent with Bragg's Law. By successfully screening the electrostatic force, the neighboring magnetic particles are separated by the rigid solvation layer immobilized on the silica surfaces, producing repulsive forces that balance the magnetically induced dipole interparticle attraction. The thicknesses of the solvation layers, as estimated by calculating the interparticle separation through the Bragg equation, were found to be consistent with literature values obtained by other force measurement methods.[9,13] The hydrogen bonding ability of the solvents was found to be an important factor that determines the thickness of the solvation layer. When water was gradually replaced by alcohols with relatively weaker hydrogen bonding abilities, the hydrogen bonding network was interrupted, resulting in thinner solvation layers, with the thickness of the solvation layer decreasing more for alcohols with longer carbon chains. We believe this magneto-photonic method represents a simple yet very effective tool for studying many types of short-range colloidal interactions including not only the solvation forces between various surfaces but also the steric effects which are fundamentally critical to chemistry, biochemistry, and pharmacology.

MATERIALS AND METHODS

Materials. Ethanol, anhydrous ferric chloride ($FeCl_3$), ammonium hydroxide solution, tetraethyl orthosilicate (TEOS), glycerol, ethylene glycol, isopropyl alcohol, methanol, and sodium hydroxide (NaOH) were purchased from Fisher Scientific. Polyacrylic acid (PAA, MW = 1800) and diethylene glycol (DEG) were obtained from Sigma-Aldrich. Distilled water was used in all experiments. All chemicals were directly used as received without further treatment.

Synthesis of Fe_3O_4@SiO_2. In a typical synthesis, a mixture of 4 mmol PAA, 0.4 mmol $FeCl_3$, and 17 mL of DEG was heated at 220 °C under nitrogen protection for 1 h. After injection of 1.75 mL of NaOH/DEG solution (2.5 mol/L), the solution was further heated for 1 h at 220 °C, and then cooled down to room temperature. Upon being cleaned with a mixture of water and ethanol several times, Fe_3O_4 CNCs were dispersed in 3 mL of water, mixed sequentially with 1 mL of ammonium hydroxide solution, 20 mL of ethanol, and 200 μL of TEOS under mechanical stirring. After reacting for 40 min, the Fe_3O_4@SiO_2 particles were cleaned with ethanol for a few times and finally dispersed in 3 mL of different solvents. The Fe_3O_4@SiO_2 particles were washed three times before being transferred to a different solvent.

Characterization. The morphology of the Fe_3O_4@SiO_2 colloids was characterized using a Tecnai T12 transmission electron microscope (TEM). The measurement of refractive indices of the solvents at 589 nm was performed using an Abbe refractometer. The UV—vis spectra were measured by a probe-type Ocean Optics HR2000CG-UV—vis spectrophotometer in reflection mode with an integration time of 700 ms. A Zeiss AXIO Imager optical microscope connected to a digital camera was used to observe the *in situ* assembly of Fe_3O_4@SiO_2 colloids. Magnets were placed underneath the sample stage and could be manually moved vertically to change the magnet—sample distance.

Conflict of Interest: The authors declare no competing financial interest.

Acknowledgment. We thank the U.S. Army Research Laboratory for support of this research (Award No: W911NF-10-1-0484). Yin also thanks the Research Corporation for Science Advancement for the Cottrell Scholar Award, 3M for the Nontenured Faculty Grant, and DuPont for the Young Professor Grant.

Supporting Information Available: Refractive indices of various solvents. This material is available free of charge *via* the Internet at http://pubs.acs.org.

REFERENCES AND NOTES

1. Derjaguin, B. On the Repulsive Forces between Charged Colloid Particles and on the Theory of Slow Coagulation and Stability of Lyophobe Sols. *Trans. Faraday Soc.* **1940**, *35*, 203–215.
2. Derjaguin, B. V.; Landau, L. *USSR Acta Physicochim* **1941**, *14*, 633.
3. Verwey, E. J.; Overbeek, J. T. G. *Theory of the Stability of Lyophobic Colloids*; Elsiever: New York, 1947.
4. Depasse, J.; Watillon, A. The Stability of Amorphous Colloidal Silica. *J. Colloid Interface Sci.* **1970**, *33*, 430–438.
5. Yotsumoto, H.; Yoon, R.-H. Application of Extended DLVO Theory: I. Stability of Rutile Suspensions. *J. Colloid Interface Sci.* **1993**, *157*, 426–433.
6. Derjaguin, B. V.; Churaev, N. V. Structural Component of Disjoining Pressure. *J. Colloid Interface Sci.* **1974**, *49*, 249–255.
7. Churaev, N. V.; Derjaguin, B. V. Inclusion of Structural Forces in the Theory of Stability of Colloids and Films. *J. Colloid Interface Sci.* **1985**, *103*, 542–553.

8. Horn, R. G.; Smith, D. T.; Haller, W. Surface Forces and Viscosity of Water Measured between Silica Sheets. *Chem. Phys. Lett.* **1989**, *162*, 404–408.
9. Grabbe, A.; Horn, R. G. Double-Layer and Hydration Forces Measured between Silica Sheets Subjected to Various Surface Treatments. *J. Colloid Interface Sci.* **1993**, *157*, 375–383.
10. Vigil, G.; Xu, Z.; Steinberg, S.; Israelachvili, J. Interactions of Silica Surfaces. *J. Colloid Interface Sci.* **1994**, *165*, 367–385.
11. Besseling, N. A. M. Theory of Hydration Forces between Surfaces. *Langmuir* **1997**, *13*, 2113–2122.
12. Manciu, M.; Ruckenstein, E. Role of the Hydration Force in the Stability of Colloids at High Ionic Strengths. *Langmuir* **2001**, *17*, 7061–7070.
13. Valle-Delgado, J. J. Hydration Forces between Silica Surfaces: Experimental Data and Predictions from Different Theories. *J. Chem. Phys.* **2005**, *123*, 034708.
14. Tadros, T. F.; Lyklema, J. Adsorption of Potential-Determining Ions at Silica-Aqueous Electrolyte Interface and Role of Some Cations. *J. Electroanal. Chem.* **1968**, *17*, 267-&.
15. Van Megen, W.; Snook, I.; Overbeek, J. T. G.; Silberberg, A.; Levine, S.; White, J. W.; Verwey, E. J. W.; Israelachvili, J. N.; Lyklema, J.; Ottewill, R. H.; *et al*. General Discussion. *Faraday Discuss. Chem. Soc.* **1978**, *65*, 43–57.
16. Bailey, J. R.; McGuire, M. M. ATR−FTIR Observations of Water Structure in Colloidal Silica: Implications for the Hydration Force Mechanism. *Langmuir* **2007**, *23*, 10995–10999.
17. Eun, C.; Berkowitz, M. L. Origin of the Hydration Force: Water-Mediated Interaction between Two Hydrophilic Plates. *J. Phys. Chem. B* **2009**, *113*, 13222–13228.
18. Yoon, R.-H.; Vivek, S. Effects of Short-Chain Alcohols and Pyridine on the Hydration Forces between Silica Surfaces. *J. Colloid Interface Sci.* **1998**, *204*, 179–186.
19. Raghavan, S. R.; Walls, H. J.; Khan, S. A. Rheology of Silica Dispersions in Organic Liquids: New Evidence for Solvation Forces Dictated by Hydrogen Bonding. *Langmuir* **2000**, *16*, 7920–7930.
20. Ducker, W. A.; Senden, T. J.; Pashley, R. M. Direct Measurement of Colloidal Forces Using an Atomic Force Microscope. *Nature* **1991**, *353*, 239–241.
21. Bibette, J. Monodisperse Ferrofluid Emulsions. *J. Magn. Magn. Mater.* **1993**, *122*, 37–41.
22. Calderon, F. L.; Stora, T.; Mondain Monval, O.; Poulin, P.; Bibette, J. Direct Measurement of Colloidal Forces. *Phys. Rev. Lett.* **1994**, *72*, 2959.
23. Dreyfus, R.; Lacoste, D.; Bibette, J.; Baudry, J. Measuring Colloidal Forces with the Magnetic Chaining Technique. *Eur. Phys. J. E* **2009**, *28*, 113–123.
24. Koenig, A.; Hebraud, P.; Gosse, C.; Dreyfus, R.; Baudry, J.; Bertrand, E.; Bibette, J. Magnetic Force Probe for Nanoscale Biomolecules. *Phys. Rev. Lett.* **2005**, *95*, 128301.
25. Dimitrova, T. D.; Leal-Calderon, F. Forces between Emulsion Droplets Stabilized with Tween 20 and Proteins. *Langmuir* **1999**, *15*, 8813–8821.
26. Ge, J.; Hu, Y.; Yin, Y. Highly Tunable Superparamagnetic Colloidal Photonic Crystals. *Angew. Chem., Int. Ed.* **2007**, *119*, 7572–7575.
27. Ge, J.; Yin, Y. Magnetically Tunable Colloidal Photonic Structures in Alkanol Solutions. *Adv. Mater.* **2008**, *20*, 3485–3491.
28. Ge, J.; Lee, H.; He, L.; Kim, J.; Lu, Z.; Kim, H.; Goebl, J.; Kwon, S.; Yin, Y. Magnetochromatic Microspheres: Rotating Photonic Crystals. *J. Am. Chem. Soc.* **2009**, *131*, 15687–15694.
29. Kim, H.; Ge, J.; Kim, J.; Choi, S.; Lee, H.; Lee, H.; Park, W.; Yin, Y.; Kwon, S. Structural Colour Printing Using a Magnetically Tunable and Lithographically Fixable Photonic Crystal. *Nat. Photon.* **2009**, *3*, 534–540.
30. Ge, J.; Yin, Y. Responsive Photonic Crystals. *Angew. Chem., Int. Ed.* **2011**, *50*, 1492–1522.
31. Ge, J.; Hu, Y.; Biasini, M.; Beyermann, W. P.; Yin, Y. Superparamagnetic Magnetite Colloidal Nanocrystal Clusters. *Angew. Chem.* **2007**, *119*, 4420–4423.
32. Ge, J.; Hu, Y.; Zhang, T.; Huynh, T.; Yin, Y. Self-Assembly and Field-Responsive Optical Diffractions of Superparamagnetic Colloids. *Langmuir* **2008**, *24*, 3671–3680.
33. Ge, J.; Yin, Y. Magnetically Responsive Colloidal Photonic Crystals. *J. Mater. Chem.* **2008**, *18*, 5041–5045.
34. Ren, J.; Song, S.; Lopez-Valdivieso, A.; Shen, J.; Lu, S. Dispersion of Silica Fines in Water−Ethanol Suspensions. *J. Colloid Interface Sci.* **2001**, *238*, 279–284.
35. Song, S. X.; Song, S. X.; Peng, C. S. Thickness of Solvation Layers on Nano-Scale Silica Dispersed in Water and Ethanol. *J. Dispersion Sci. Technol.* **2005**, *26*, 197–201.
36. Russel, W. B., Saville, D. A. Schowalter, W. R. *Colloidal Dispersions*; Cambridge University Press: Cambridge, UK, 1989.
37. Ott, J. B.; Goates, J. R.; Lamb, J. D. Solid-Liquid Phase Equilibria in Water + Ethylene Glycol. *J. Chem. Thermodyn.* **1972**, *4*, 123–126.
38. Cordray, D. R.; Kaplan, L. R.; Woyciesjes, P. M.; Kozak, T. F. Solid−Liquid Phase Diagram for Ethylene Glycol + Water. *Fluid Phase Equilib.* **1996**, *117*, 146–152.
39. Dean, J. A. *Lange's Handbook of Chemistry,* 15th ed.; McGraw-Hill: New York, 1999.